

広島大学学術情報リポジトリ
Hiroshima University Institutional Repository

Title	Effect of conical length on separation performance of sub-micron particles by electrical hydro-cyclone
Author(s)	Yoshida, Hideto; Hayase, Yuuki; Fukui, Kunihiro; Yamamoto, Tetsuya
Citation	Powder Technology , 219 : 29 - 36
Issue Date	2012
DOI	10.1016/j.powtec.2011.12.002
Self DOI	
URL	http://ir.lib.hiroshima-u.ac.jp/00034792
Right	(c) 2012 Elsevier B.V. All rights reserved.
Relation	



“Effect of conical length on separation performance of sub-micron particles by electrical hydro-cyclone”

Hideto YOSHIDA*, Yuuki HAYASE, Kunihiro FUKUI
and Tetsuya MAMOTO

Department of Chemical Engineering, Hiroshima
University, 1-4-1, Kagamiyama Higashi-Hiroshima,
Hiroshima, 739-8527, Japan

The name and address of the author responsible:

Hideto Yoshida

Department of Chemical Engineering, Hiroshima Universit
y, 1-4-1, Kagamiyama Higashi-Hiroshima,
Hiroshima, 739-8527, Japan

Tel. +81-82-424-7853 FAX +81-82-424-5494

e-mail r736619@hiroshima-u.ac.jp

“Effect of conical length on separation performance of sub-micron particles by electrical hydro-cyclone”

Key Words: Hydro-cyclone, Electrostatic enhance, Beads mill, Sub micron Silica, particle separation

Abstract

Experimental studies have been carried out to assess the effect of conical section length on the performance of particle separation using an electrical hydro-cyclone. With the pre-treatment of beads by milling process, the negative zeta potential of particles increases with the increase of particle diameter.

Sub-micron particle classification was possible by use of the special electrical hydro-cyclone under electrical potential of less than 150V and an inlet flow rate of less than 0.3l/min. Due to the increase of particle residence time in the cyclone, the 50% cut size decreases with the increase of conical section length. The partial separation efficiency increases with the increase of applied potential or the decrease of inlet flow rate.

The experimental data agreed with the proposed model assuming constant surface charge density of particles.

1. Introduction

Hydro-cyclone separators have been widely used as solid-liquid separation apparatus because they are simple in construction, require low operating and maintenance costs and can be used under a wide range of operating conditions [1,2]. Recent interest in hydro-cyclone separation has focused on separation of particles in the sub-micron region with a fairly high degree of classification, since the particles with such a size range (0.1 to $1\mu\text{m}$) are required for various powder handling processes. Several techniques of flow controlling method at the outlet pipe of the hydro-cyclone were reported [3,4], and some new methods of controlling the cut size of the hydro-cyclone by modifying the inlet section have been developed [5,6]. Estimations for a 50% cut in size for hydro-cyclones have been obtained via various approaches [7, 8, 9, 10].

In order to enhance the separation performance of gas cyclones without increasing their pressure drop, the use of additional applied potential has been examined, and the effect of various operating conditions and dimensions on the separation

performance of electrically enhanced gas cyclones have been reported [11,12,13]. Several models predicting the separation performance of an electrically enhanced gas cyclone have been built [14,15]. Compared with those of electrical gas cyclones, fewer studies have been carried out regarding the effect of applied external electrostatic potential on the separation performance of the hydro-cyclone. Since the dimensions of most hydro-cyclones are smaller than those of gas cyclones, and the dielectric constants of liquids are much larger when compared with those of gases, smaller applied electrostatic potential, which leads to less energy consumption, can be applied in order to increase the classification performance of fine particles. The first work about electrical hydro-cyclones was reported by Yoshida *et al.* [16]. The minimum cut size achieved by use of the typical laboratory scale hydro-cyclone is about $5\mu\text{m}$ under normal operating conditions and $3\mu\text{m}$ under high pressure conditions. By using multiple inlets, the cut size could be reduced to about $2\mu\text{m}$ [17]. However, the typical hydro-cyclone, which depends only on the tangential force, is unable to separate

the sub-micron particles. In order to separate the sub-micron particles, an additional force should be applied within the apparatus. Our previous study indicates that by use of a special electrical hydro-cyclone under low flow rates, the achieved cut size was about $0.4\mu\text{m}$ [18,19].

This paper describes the effect of conical section length of the special electrical hydro-cyclone on the separation performance of the sub-micron particles. A simple model based on the diffusive mass transfer mechanism in the conical section is proposed in order to estimate the separation performance. The new type of outlet pipe, aimed to increase the separation performance, is also proposed and the performance examined experimentally with some interesting results obtained.

2 Experimental methods

The experimental apparatus of the electrical hydro-cyclone is shown in Figure 1. The system in general, consists of a hydro-cyclone with a 20% under-flow ratio and a suspension mixing tank. Well-dispersed 0.5wt% of silica suspension was pumped into the hydro-cyclone with low flow rates, since only the effect

of the electrostatic force on the separation performance of the special electrical hydro-cyclone, not the inertial force, was considered as the main driving force of separation in the hydro-cyclone. The temperature of the feed suspension was controlled to 30°C. The samples of both fine and coarse suspensions were collected, and the mass of each sample was measured.

The Dynamic Light Scattering method (HORIBA Co. Ltd., LB-550) was used as the particle size distribution analyzer, and the zeta potential of the suspension was measured by use of a zeta potential measuring device (Zetasizer 2000, Malvern Instrument Co. Ltd.). The partial separation efficiency, $\Delta\eta$, was calculated by:

$$\Delta\eta = \frac{m_c f_c \Delta D_p}{m_c f_c \Delta D_p + m_s f_s \Delta D_p} \quad (1)$$

In the above equation, m_c and m_s represent the masses of the dried collected particles, while f_c and f_s are the particle size distributions of coarse and fine sides, respectively.

A 20mm diameter hydro-cyclone was employed in this study, a center rod with a 2mm diameter was inserted vertically inside the conical part, and the test section was electrically insulated from

both the circular inlet and under-flow box sections. The electrical hydro-cyclones with different conical lengths, 120, 180 and 240 mm, were used in the experiments.

Since the silica particles in the suspension are negatively charged inside an electrostatic field, in order to achieve separation by use of electrostatic force, the center rod should be controlled as the negative electrode and the conical wall as the positive one. Both the center electrode and the wall of the conical section were connected to a DC power generator. The generated electrostatic field caused by the potential difference between the wall of conical section and center electrode enables the movement of negatively charged silica particles toward the wall of the conical section.

Sub-micron silica particles with a $0.2\mu\text{m}$ median diameter and specific surface area of $22.7\text{m}^2/\text{g}$ were used as the test powder. The true density of the particles is $2.2\text{g}/\text{cm}^3$, and their size distribution is shown in Figure 2.

A beads mill (UAM-015, Kotobuki Industries Co. Ltd.) was used as the method of particle dispersing before the separation

experiment. Beads milling method was selected because it is effective in dispersing the sub-micron particles, and can increase the zeta potential of the particles. The sub-micron silica particles suspended in the ion exchanged water were supplied into the vessel under a closed loop beads mill system. In the milling vessel, the agglomerated fine particles were dispersed into their primary sizes by the beads. The beads and the remaining agglomerated particles were removed from the suspension in the upper part of vessel by centrifugal force. The well-dispersed suspension was then recycled back into the suspension tank. The milling process was carried out within 30min. After the process was finished, the suspension was immediately used for separation experiments. After the beads mill process, the suspension was supplied to the slurry tank and flow control was carried out in about 5min without applying the electrical potential. Then, the separation experiment with the electrical potential was started and the samples of over-flow and under-flow were collected into the different vessels.

3 Experimental Results and Discussion

3-1 Preparation of feed slurry solution

In order to carry out sub-micron particle classification, it is important to disperse the agglomerated particles into their primary particles. Before the separation experiment, the particle dispersion state was examined by use of SEM observation. The two kinds of silica beads of 100 and 150 μ m were used in the beads milling process. The milling time was 30min. and a tangential velocity of 6.65m/s was selected for the beads milling condition. Figure 3. shows the particles after the treatment of beads milling. It is found that some particles are broken in the case of the 150 μ m beads. Due to the strong centrifugal field, the sub-micron silica particles were affected more by the centrifugal force for the 150 μ m beads. However, the broken particles are not observed in the case of 100 μ m silica beads. The particle size distribution with 100 μ m beads is smaller than that of the 150 μ m beads. Then the 100 μ m silica beads were selected for the beads milling process.

The relationship between the median particle diameter and zeta potential is shown in Figure 4. The data was obtained by use of

the forced centrifugal separator, under the different rotational speeds of 10000-15000rpm. Larger particles are subjected to a greater negative charging, compared with the smaller ones. An increase in the particle diameter means an increase in the interfacial area between suspended particles and the bulk liquid. Higher interfacial area implies a larger number of ions attached to the surface of the particles. Consequently, the larger particles have greater electrical mobility compared to the smaller ones in an electrostatic field. In the electrical hydro-cyclone, the larger particles might be collected at the positive electrode (the conical wall) and then move down through the lower outlet orifice. The drag force from the liquid would exceed the electrostatic force of smaller particles, and they would move through the upper outlet pipe. Hence, the separation of the sub-micron particles in the electrical hydro-cyclone can be achieved only by use of electrostatic force.

3-2 Experimental data of different length of conical section

In order to examine the length of conical section on the separation performance of the electrical hydro-cyclone, the

experiments were carried out using conical sections with differing lengths of 120,180 and 240mm, respectively. For the feed particle size distribution shown in Fig.2, it is very difficult to separate the sub-micron particles without applying the electrical potential in the hydro-cyclone.

Figure 5 shows the experimental data for the conical length of 120mm. The 50% cut size decreases as the inlet flow rate decreases. The particle residence time increases as the inlet flow rate decreases, affecting the particles for a longer time during the electric classification process. It is also found that the 50% cut size decreases as the electric potential increases. The radial particle velocity increases with the increase of electrical potential, so that the collection efficiency of under-flow side increases as the electrical potential increases. Figure 6 shows the experimental data for the conical length of 180mm. Compared to the data shown in Fig.5, the 50% cut size changes are smaller than those for the conical length of 120mm. For example, the 50% cut size changes from 0.28 to 0.38 μ m under electrical potential of 100V and conical length of 180mm. But the 50% cut

size changes from 0.32 to 0.42 μ m for the data shown in Fig.5. Because particle residence time increases with an increase in the conical length, particles are affected more chance of electrical classification process. Therefore, a decrease of the 50% cut size is obtained in the case of the longer conical length.

Figure 7 shows the data for the conical length of 240mm. Compared to the previous Figs.5 and 6, the 50% cut size changes are smaller than those in the other two cases. The 50% cut size changes from 0.23 to 0.36 μ m under each of the three kinds of flow rate with electrical potential of 100V. Comparing Figs.5 to 7, it is generally found that the 50% cut size decreases as the inlet flow rate decreases or the electrical potential increases.

3-3 Improvement of separation performance

In order to decrease the 50% cut size, the experimental conditions of low flow rate and longer conical length are recommended. However for the case of conical length of 240mm, the low inlet flow rate may be considered as the driving force of its directional change from downward to upward in the region of

conical section. In order to overcome this difficulty, the newly developed special ring shown in Fig.8 was used for the experiments of the cyclone with conical length of 240mm. The entire inlet flow tends to move to the lower conical section with the use of the ring shown in Fig.8, compared to the case without the ring. Two types of ring of differing sizes were used in the separation experiments.

Figure 8 shows the experimental data of particle separation both with and without the special ring under the applied electrical potential of 100V, inlet flow rate of 0.1l/min and conical length of 240mm. The 50% cut size change is smaller and classification accuracy increases for the case of the type B ring. The length of h in the type B ring is longer than that in the type A ring, then the inlet flow tends to move to the lower conical section for the type B ring. The effect of the ring on particle separation performance was clearly found for the cyclone with conical length of 240mm, and this effect decreased for the cyclones with shorter conical length.

4 Proposed model

The experimental results without electrical potential indicated particle classification is difficult in low flow rate region, then hydrodynamic effect is not included in the proposed model.

In order to predict the partial separation efficiency of the electrical hydro-cyclone when considering particle collection mechanisms of the electrical and diffusion phenomena, a simplified model shown in Fig.9 is applied. The following assumptions are used in the proposed model.

- (1) The conical section of the hydro-cyclone is simplified to the coaxial cylindrical section with the inside electrode radius of R_i and outer wall radius of R .
- (2) In the axial direction, the particle velocity is equal to the fluid velocity and radial mixing of particles is considered.
- (3) Particle surface charge density is assumed to be constant for various particle diameters.

4-1 Collection efficiency by electrical force

As shown in Fig.4, the zeta potential decreases with the increase of particle diameter, then the negative particle charge of a particle increases as the particle diameter increases. The particle electrical mobility μ_e is defined as follows:

$$\mu_e = \frac{q}{3 \pi \mu D_p} = \frac{\pi D_p^2 \sigma}{3 \pi \mu D_p} = \frac{D_p \sigma}{3 \mu} \quad (2)$$

where σ indicates surface charge density of particles.

The radial velocity of particle v_r is obtained by the following equation:

$$v_r = \mu_e E_r = \frac{D_p \sigma 10^7}{3 \mu} E_r \quad (3)$$

The value of E_r indicates electrical field strength in the radial direction and is calculated by the following equation:

$$E_r = -\frac{\partial V}{\partial r} = -\frac{\Delta V}{r \ln\left(\frac{R}{R_i}\right)} \quad (4)$$

Substituting Eq.(4) into Eq.(3), and r equal to $R/2$, the radial particle velocity is obtained by the following equation:

$$v_r = \frac{D_p \sigma 10^7 (-\Delta V)}{3 \mu \frac{R}{2} \ln\left(\frac{R}{R_i}\right)} \quad (4)$$

Considering radial mixing of particle, where S and Q* are area of particle collection and volume flow rate respectively, the partial separation efficiency of the electrical force is derived as follows:

$$\Delta \eta_e = 1 - \exp\left(-\frac{S v_r}{Q^*}\right) \quad (6)$$

The values of S and Q* are calculated by the following equations:

$$S = 2 \pi R \Delta z \quad R = \frac{(R_1 + R_2)}{2} \quad (7)$$

$$Q^* = \frac{(Q + Q B_d)}{2} \quad (8)$$

Then the dimensionless parameter $(S v_r / Q^*)$ in Eq.(6) is simplified as follows:

$$\frac{S v_r}{Q^*} = \frac{2 \pi R \Delta z D_p \sigma 10^7 (-\Delta V)}{Q^* 3 \mu \frac{R}{2} \ln\left(\frac{R}{R_i}\right)} = \frac{4 \pi \Delta z 10^7 D_p \sigma (-\Delta V)}{3 \mu Q^* \ln\left(\frac{R}{R_i}\right)} = \frac{K_1 D_p \sigma (-\Delta V)}{Q^*} \quad (9)$$

The value of K₁ is defined by the following equation:

$$K_1 = \frac{4 \pi \Delta z 10^7}{3 \mu \ln \left(\frac{R}{R_i} \right)} \quad (10)$$

Substituting Eq.(9) into Eq.(6), the collection efficiency by electrical force can be calculated:

$$\Delta \eta_e = 1 - \exp \left(- \frac{K_1 D_p \sigma (-\Delta V)}{Q^*} \right) \quad (11)$$

4-2 Collection efficiency by particle diffusion

The partial separation efficiency due to particle diffusion is derived as follows in our previous paper [19]:

$$\Delta \eta_d = 1 - \exp \left(- \frac{K_2 D}{Q^*} \right) \quad (12)$$

where the parameter K_2 is defined as follows:

$$K_2 = \left(\frac{8 \pi \Delta z}{\frac{(R_i^2 + R^2)}{(R_i^2 - R^2)} + \frac{1}{\ln \left(\frac{R_i}{R} \right)}} \right) \quad (13)$$

In Eq.(12), D is the Brownian diffusion coefficient defined by the following equation:

$$D = \frac{k T}{3 \pi \mu D_p} \quad (14)$$

4-3 Total collection efficiency due to electrostatic force and particle diffusion mechanisms

To combine the partial separation efficiency of both mechanisms, the following equation is derived:

$$\Delta\eta_t = \Delta\eta_e + (1 - \Delta\eta_e) \Delta\eta_d \quad (15)$$

Substituting Eqs.(6),(9),(12) into Eq.(15), the total partial separation efficiency considering the electrostatic and diffusion mechanisms is derived as follows:

$$\Delta\eta_t = 1 - \exp\left(-\frac{K_1 D_p \sigma (-\Delta V) + K_2 D}{Q^*}\right) \quad (16)$$

For the particles with both mechanisms ignored, the total partial separation efficiency approaches to the constant value B_c . Then corrected partial separation efficiency is finally obtained in the following equation:

$$\Delta\eta_c = B_c + (1 - B_c) \Delta\eta_t = B_c + (1 - B_c) \left(1 - \exp\left(-\frac{K_1 D_p \sigma (-\Delta V) + K_2 D}{Q^*}\right)\right) \quad (17)$$

In Eq.(17), the only unknown parameter is the surface charge density σ . The value of σ can be found by fitting the calculated

results to the experimental data, with the value of σ as a fitting parameter. The least square method was used to find out the optimum specific charge density of particle.

5 Effect of applied potential on separation performance

In order to examine the effect of electrostatic potential on the separation performance of electrical hydro-cyclone, experiments under various electrostatic potential conditions, ranging from 50 to 150V, were carried out. , Figure 10-1 shows the experimental results for the conical length of 120mm. The separation performance increases under the higher applied potential. The 100% cut size is shifted to the smaller particle diameter under the applied potential of 150V, compared to the conditions of 50V and 100V. The strength of the electrostatic field between the center rod and the conical wall increases with rising applied electrostatic potential. The increase of the electrostatic field causes an increase in the radial migration velocity of particles, and finally the increase of particle collection efficiency. The lines shown in the figure indicate the calculated results under the specific surface charge density of $-2.9 \times 10^{-6} \text{C/cm}^2$. The experimental results agree well with the calculated results. Figures 10-2 and 10-3 show the experimental results for the conical length of 180mm and 240mm, respectively. In these cases, the 50% cut size decreases as electrical potential increases and the experimental results agree with the calculated ones. Under

the same electrical potential, the 50% cut size decreases with the increase of the conical length. Because the particles are affected by more chance of the separation for the conical length of 240mm, the 50% cut size is the lowest of the three cases.

6 Effect of inlet flow rate on the separation performance

In order to examine the effect of inlet flow rate on the separation performance of the electrical hydro-cyclone, the experiments were carried out for a flow rate of 0.1, 0.2 and 0.3 l/min, respectively. The experimental results are shown in Fig.11-1 under the conical length of 120mm and electrical potential of 100V. The separation performance increases with the decrease of inlet flow rate. This phenomenon is different from the typical hydro-cyclone, in which the separation performance increases as the inlet flow rate increases. The 50% cut size corresponding to the inlet flow rate of 0.1, 0.2 and 0.3 l/min were about 0.32, 0.36 and 0.41 μm , respectively. The lower inlet flow rate means longer residence time of particles, and results in a higher particle separation performance. The lines shown in the Figures indicate the calculated results assuming the specific surface charge density of $-2.9 \times 10^{-6} \text{C/cm}^2$. The experimental results agree with the calculated ones. Figures 11-2 and 11-3 show the data for the conical length of 180 and 240mm, respectively. The same trends as shown in Fig.11-1 are observed in these two cases. Due to the increase in particle residence time in the cyclone, a 50% cut size of about 0.23 μm was obtained

under the inlet flow rate of 0.11/min and conical length of 240mm. However, deviations between the calculated results and experimental ones are found for the conical length of 240mm. In spite of the special ring attached to the outlet pipe for this cyclone, some parts of inlet flow changes its direction from downward to upward direction and the assumption used to obtain the theoretical equation might not be suitable in this case.

7 Relation between 50% cut size and inlet flow rate

In order to obtain the relationship between the 50% cut size and inlet flow rate, the all data under the electrical potential of 100V are plotted in Fig.12. The 50% cut size increases as the inlet flow rate increases or the conical length decreases. The solid lines corresponding to the three different conical length indicate the calculated results based on Eq.(17). It is found that the experimental results nearly agree with the calculated ones. By selecting a suitable operating condition, it is possible and quite effective to classify sub-micron particle by use of the special electrical cyclone proposed in this study.

Conclusions

Experimental studies about the separation performance of the special electrical hydro-cyclone have been conducted and conclusions obtained are as follows:

- (1) With the use of beads milling treatment, the negative zeta potential of sub-micron silica particle increases with the

increase of particle diameter. Sub-micron particle classification is possible with use of the special electrical hydro-cyclone.

- (2) The 50% cut size decreases with the increase of the conical length.
- (3) The partial separation efficiency increases with the increase of applied potential or the decrease of inlet flow rate.
- (4) The experimental data agree with the proposed model assuming constant surface charge density of particles.

Nomenclature

B_d : under-flow ratio	(-)
B_c : constant value	(-)
D_p : particle diameter	(μ m)
D : diffusion coefficient of particle	(cm^2/s)
E_r : strength of electrostatic field	(V/cm)
f_c, f_s : particle size distribution of coarse and fine sides, respectively	(-/ μ m)

k : Boltzman constant	(erg/K)
K_1 : constant defined by Eq.(10)	(cm^4/sCV)
K_2 : constant defined by Eq.(13)	(cm)
m_c, m_s : mass flow rate of particles for coarse and fine sides, respectively	(g/s)
q : particle charge	(C)
Q, Q^* :inlet flow rate and average flow rate, respectively	(cm^3/s)
r, z : radial and axial coordinates, respectively	(cm)
R_1, R_2 : radius of cylindrical part and bottom of conical part, respectively	(cm)
R_i, R : radius of center electrode and cylindrical pipe, respectively	(cm)
S : area of particle collection	(cm^2)
T : temperature	(K)
v_r : radial particle velocity	(cm/s)
Δz : length of conical section	(cm)
$\Delta \eta, \Delta \eta_t$: partial separation efficiency and total partial separation efficiency, respectively	(-)
$\Delta \eta_e, \Delta \eta_d$: partial separation efficiency due to electrical and diffusion mechanisms, respectively	(-)
ΔV : potential difference	(V)
μ : fluid viscosity	(Pa · s)
μ_e : electrical mobility	(cm^2/sV)
ζ : zeta potential	(mV)

σ : surface charge density (C/cm²)

References

- 1) D. Bradley, *The Hydro-cyclone*, Pergamon, London, p.1, (1965)
- 2) L. Svarovsky, *Solid-Liquid Separation*, Butterworth, New York, p.191, (2000)
- 3) L.Y. Chu, W.M. Chen, X.Z. Lee, Enhancement of hydro-cyclone performance by controlling the inside turbulence structure, *Chem. Eng. Sci.* 57, 207-212, (2002)
- 4) K. Yamamoto, X. Jiao, Hydro-cyclone with perforated inner cylinder, *Trans. Japan Soc. Mech. Eng.*, Ser. B 63,615, 133-138 (1997)
- 5) H. Yoshida , U. Norimoto and K. Fukui, Effect of blade rotation on particle classification performance of hydro-cyclone, *Powder Technol.* 164, 103-110 (2006)
- 6) H. Yoshida, S. Yoshikawa, K. Fukui, T. Yamamoto, Effect of multi-inlet flows on particle classification performance of hydro-cyclones, *Powder Technol.* 184, 352-360 (2008)
- 7) R.K. Dwari, M.N. Biswas, B.C. Meikap, Performance characteristics for particles of sand FCC and fly ash in a novel hydro-cyclone, *Chem. Eng. Sci.* 59, 671-684 (2004)
- 8) K. Nageswararao, D.M. Wiseman, T.J. Napier-Munn, Two Empirical hydro-cyclone models revisited, *Miner. Eng.* 18, 671-687 (2004)
- 9) M.A.Z. Coelho, R.A. Medronho, A Model for performance prediction of hydro-cyclones, *Chem. Eng. J.* **84**, pp 7-14, (2001)
- 10) M. Narasimha, R. Sripriya, P.K. Banerjee, CFD modeling of hydro-cyclone-prediction of cut size, *Int. J. Miner. Process.* 75, 53-68, (2001)

- 11) K.S. Lim, K.W. Lee, M.R. Kuhlman, An Experimental Study of the Performance Factors Affecting Particle Collection Efficiency of the Electro-cyclone, *Aerosol Sci. Technol.*, 35, 969-977 (2001)
- 12) G. Dodbiba, A. Shibayama, T. Miyazaki, T. Fujita, Electrostatic Separation of The Shredded Plastic Mixtures Using a Tribo-Cyclone, *Magnetic and Electrical Separation*, 11, No 1-2, 63-92 (2002)
- 13) J.S. Shrimpton, R.I. Crane, Small Electro-cyclone Performance, *Chem. Eng. Technol.*, 24 , 9, 951-955 (2001)
- 14) P.W. Dietz, Electrostatically Enhanced Cyclone Separators, *Powder Technol.* 31, 2, 221-226 (1982)
- 15) J. Li , W. Cai, Study of the Cut Diameter of Solid Gas Separation in Cyclone with Electrostatic Excitation, *Journal of Electrostatics*, 60, 15-23, (2004)
- 16) H. Yoshida, K. Fukui, W. Pratarn , W. Tanthapanichakoon, Particle Separation Performance by Use of Electrical Hydro-cyclone, *Separ. Purif. Technol.* 50, 330-335 (2006)
- 17) R.K. Tue Nenu, H. Yoshida, Comparison of Separation Performance Between Single and Two Inlets Hydro-cyclones, *Adv. Powder. Technol.* 20, 195-202 (2009)
- 18) R.K. Tue Nenu, H. Yoshida, K. Fukui, T. Yamamoto, Separation Performance of Sub-micron Silica Particles by Electrical Hydro-cyclone, *Powder. Technol.* 196, 147-155 (2009)
- 19) R.K. Tue Nenu, Y. Hayase, H. Yoshida and T. Yamamoto, Influence of inlet flow rate, pH and beads mill operating condition on separation performance of sub-micron particles by electrical hydro-cyclone, *Adv. Powder. Technol.* 21, 246-255 (2010)

Figs. & Tab. Caption

Fig.1 Experimental apparatus and electrical hydro-cyclone

Fig.2 Particle size distribution of test powder and experimental conditions

Fig.3 Particle size distribution under different dispersion conditions

Fig.4 Relationship between median size and zeta potential of particle

Fig.5 Effect of inlet flow rate and electrical potential on partial separation efficiency ($\Delta z=120$ mm)

Fig.6 Effect of inlet flow rate and electrical potential on partial separation efficiency ($\Delta z=180$ mm)

Fig.7 Effect of inlet flow rate and electrical potential on partial separation efficiency ($\Delta z=240$ mm)

Fig.8 Effect of special ring attached on upper plate on partial separation efficiency

Fig.9 Particle collection model of electrical hydro-cyclone and notations used in the proposed model

Fig.10-1 Effect of applied potential on partial separation efficiency
($\Delta z=120$ mm)

Fig.10-2 Effect of applied potential on partial separation efficiency
($\Delta z=180$ mm)

Fig.10-3 Effect of applied potential on partial separation efficiency
($\Delta z=240$ mm)

Fig.11-1 Effect of inlet flow rate on partial separation efficiency

($\Delta z=120$ mm)

Fig.11-2 Effect of inlet flow rate on partial separation efficiency

($\Delta z=180$ mm)

Fig.11-3 Effect of inlet flow rate on partial separation efficiency

($\Delta z=240$ mm)

Fig.12 Relation between 50% cut size and inlet flow rate for various conical lengths

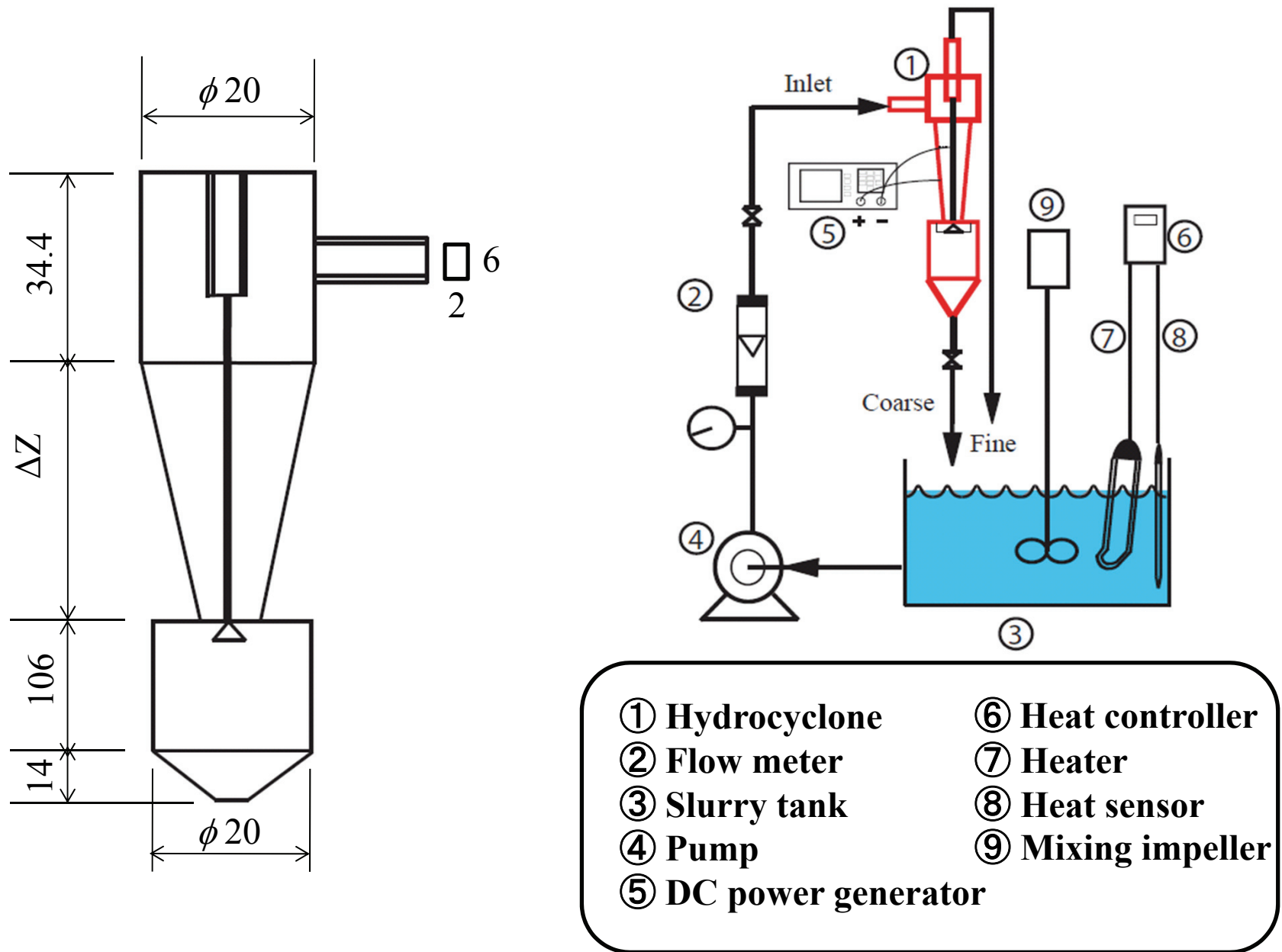
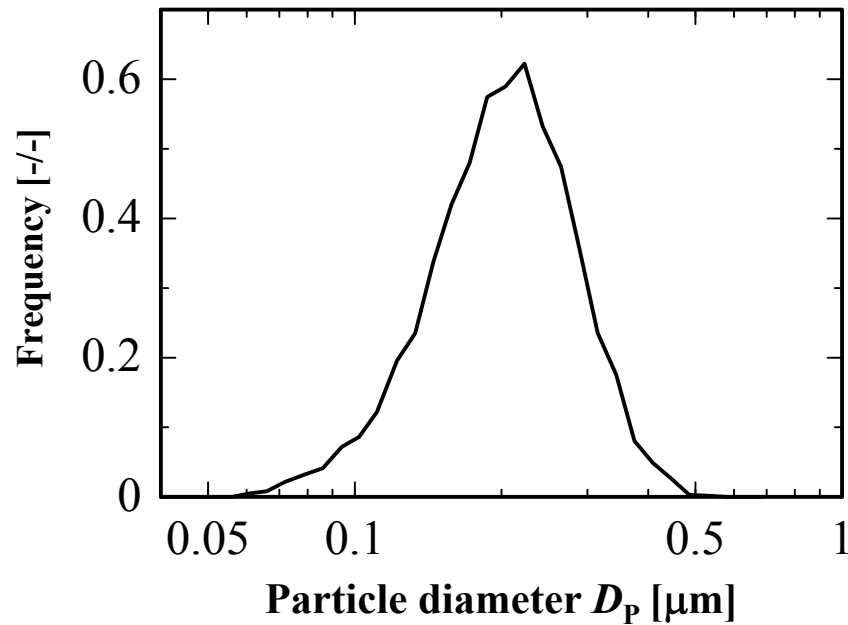
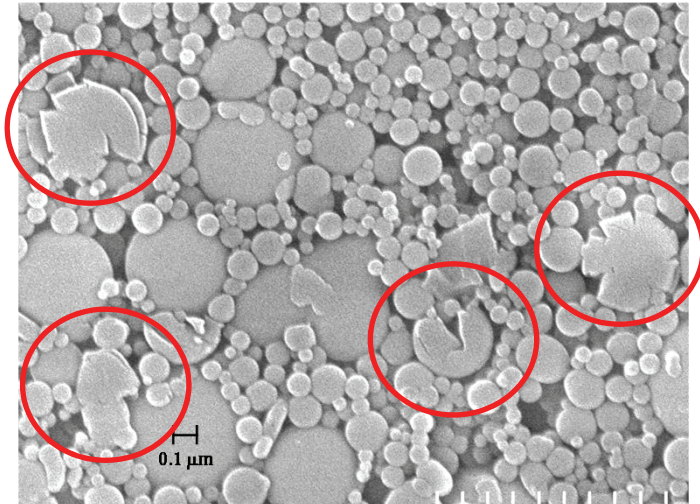


Fig.1 Experimental apparatus and electrical hydro-cyclone

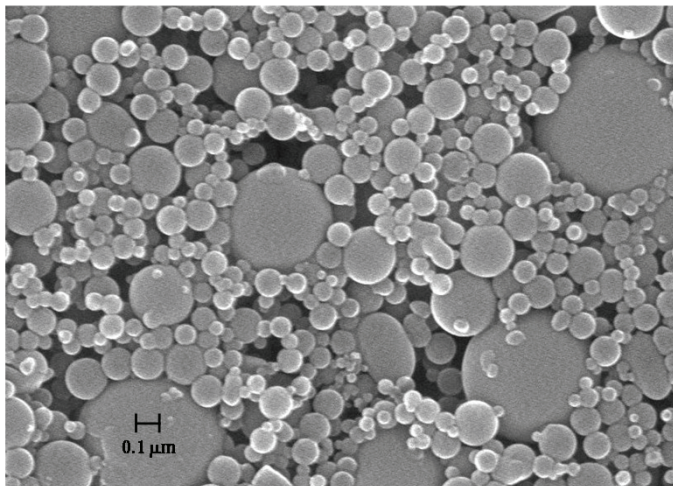


Experimental condition	
Tested powder	Silica
Density	2200 kg/m³
Dispersion medium	Ion exchanged water
Concentration of slurry	0.5 wt %
Inlet flow rate Q	0.1 ~0.3 L/min
Temperature of slurry	30 °C
Under flow ratio	20 %

Fig.2 Particle size distribution of test powder and experimental conditions



(a) 150 μm silica beads



(b) 100 μm silica beads

Beads mill condition

Milling time	30 min
circumferential velocity	6.65 m/s

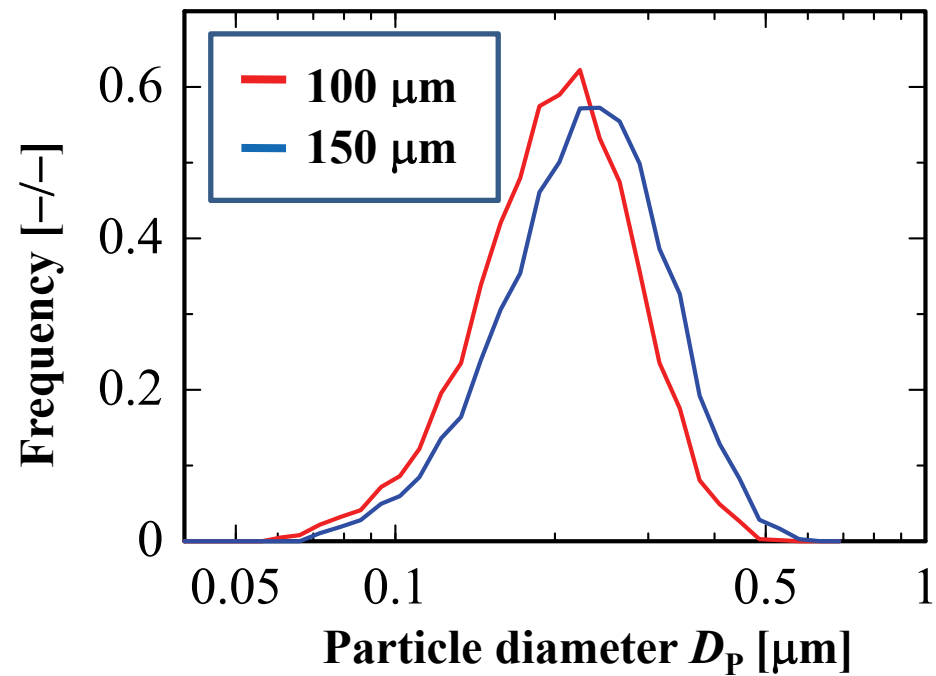


Fig.3 Particle size distribution under different dispersion conditions

Beads mill condition

Beads 100 μm silica beads
Milling time 30 min
circumferential velocity 6.65 m/s

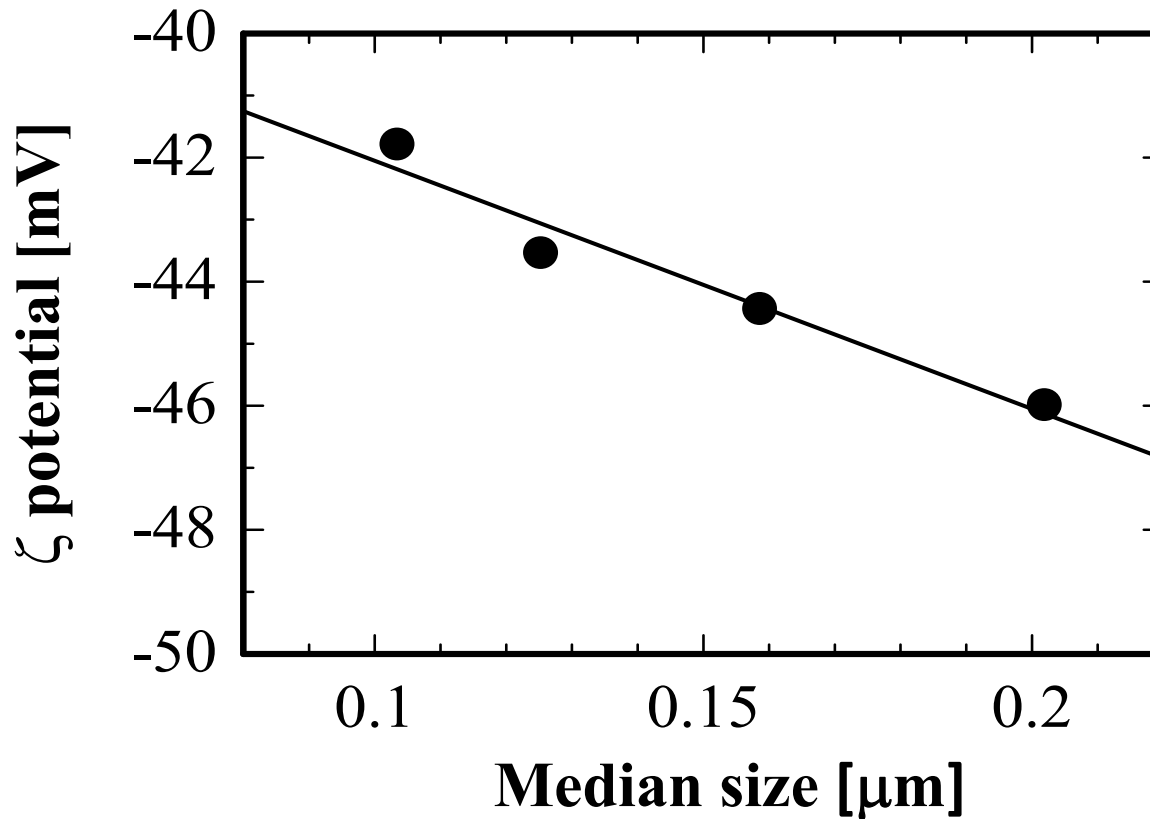


Fig.4 Relationship between median size and ζ potential of particle

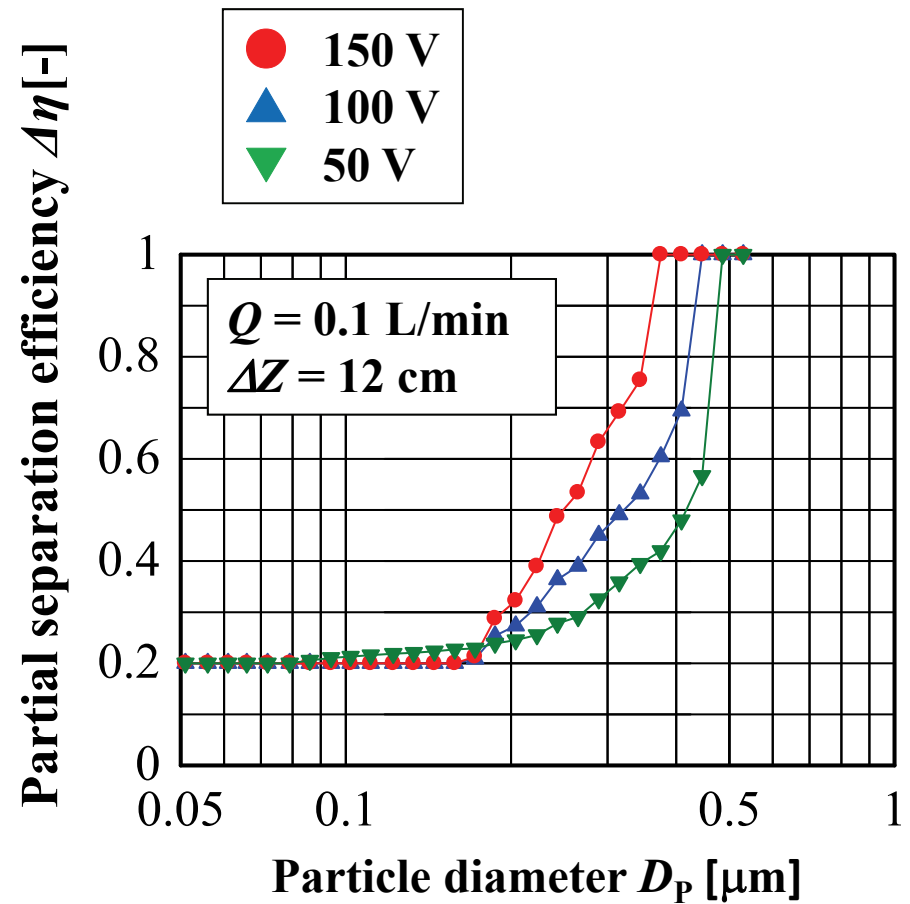
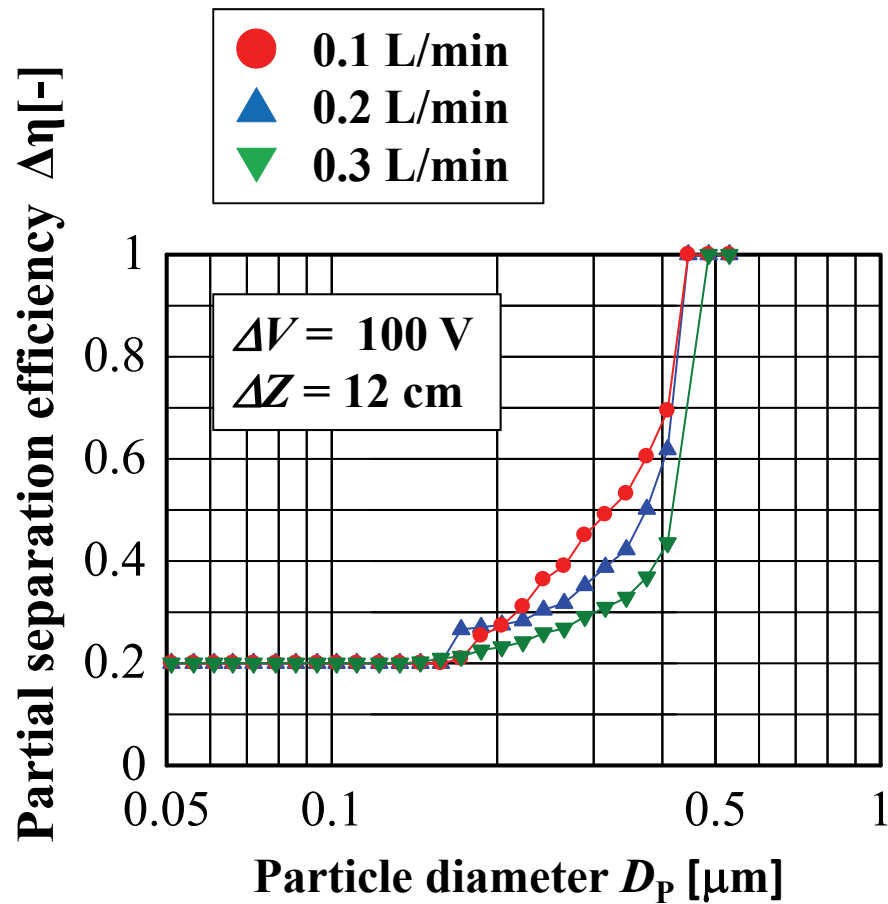


Fig.5 Effect of inlet flow rate and electrical potential on partial separation efficiency ($\Delta z=120\text{mm}$)

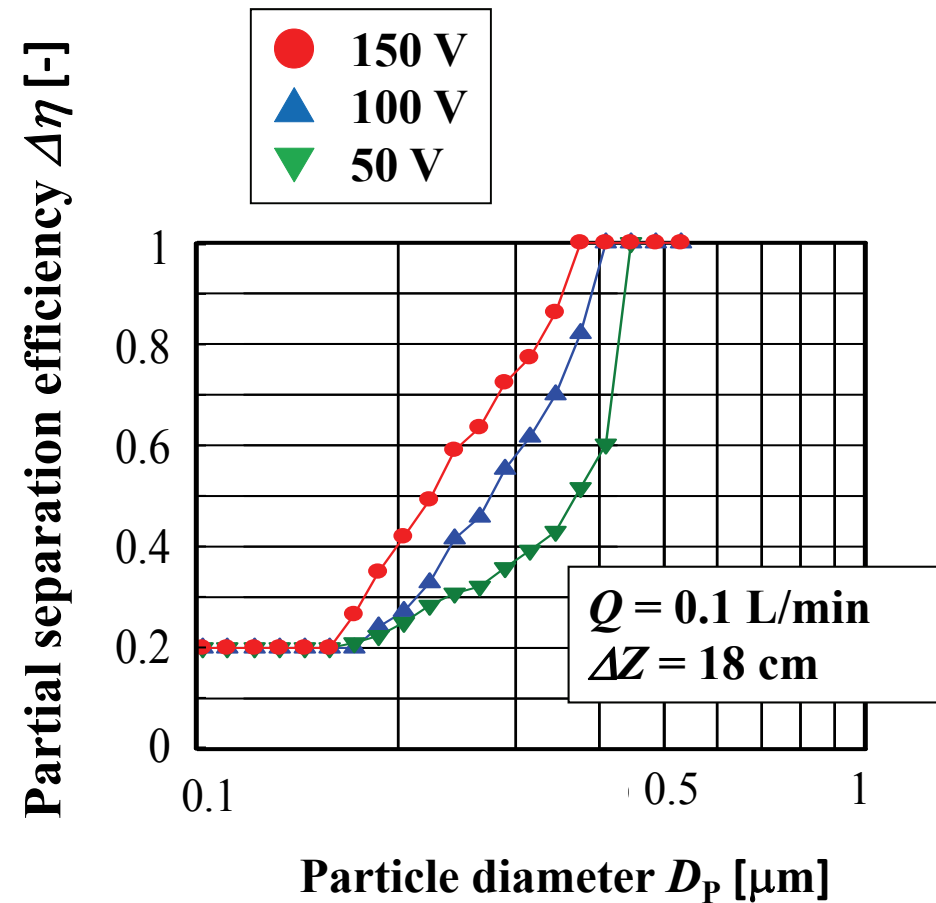
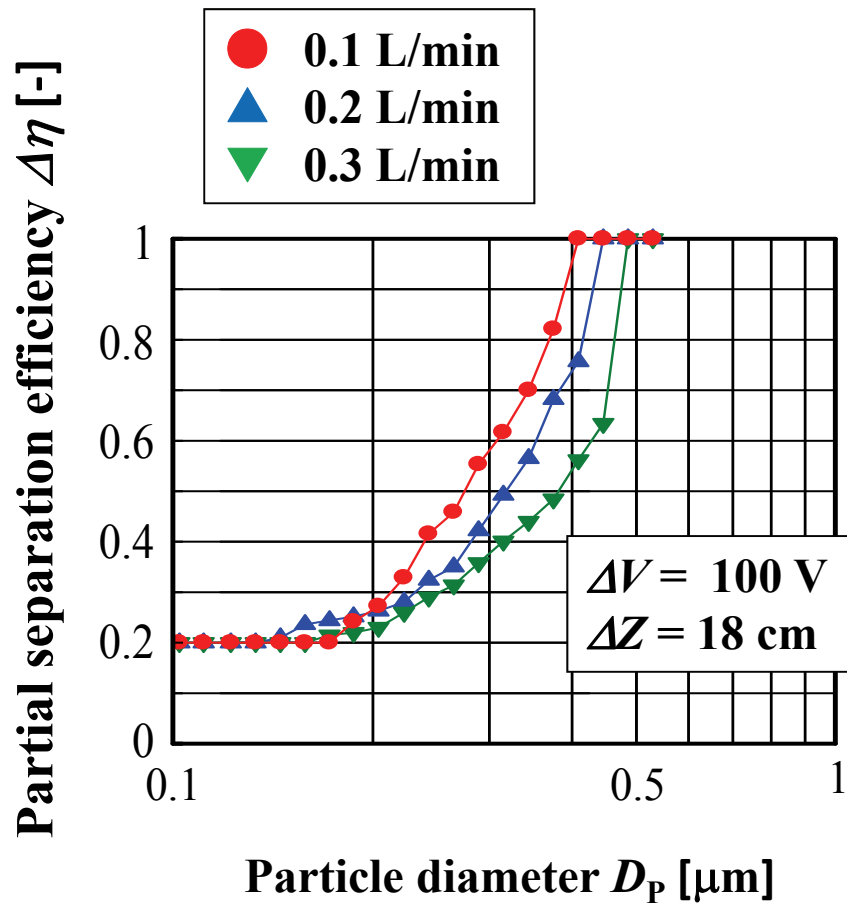


Fig.6 Effect of inlet flow rate and electrical potential on partial separation efficiency ($\Delta z=180\text{mm}$)

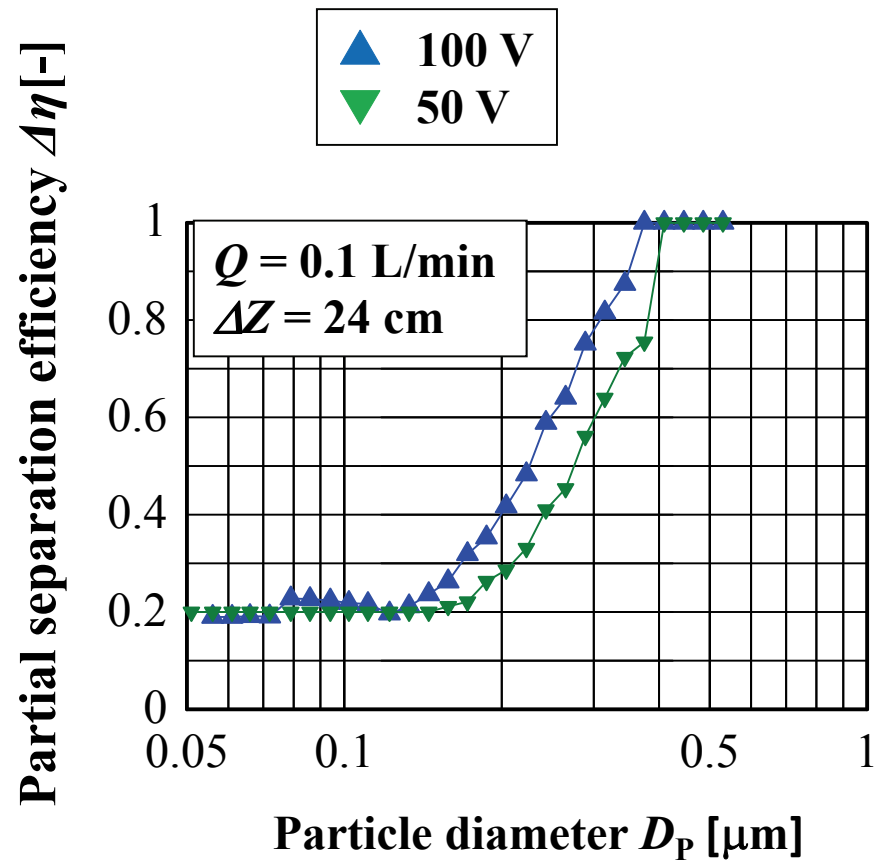
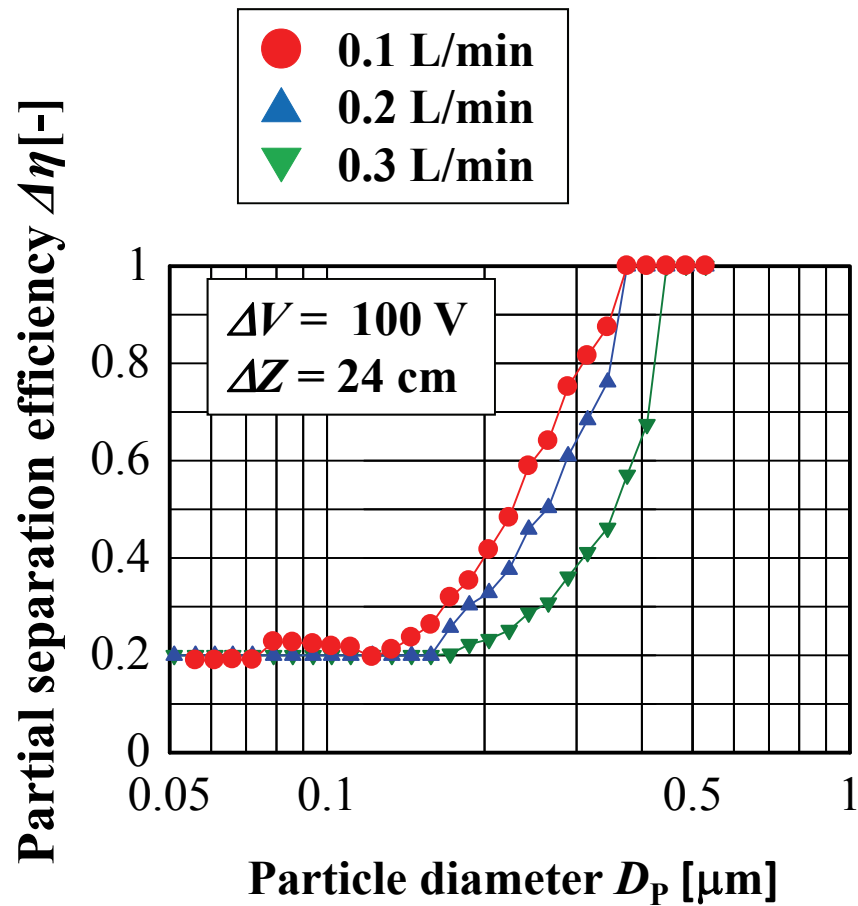
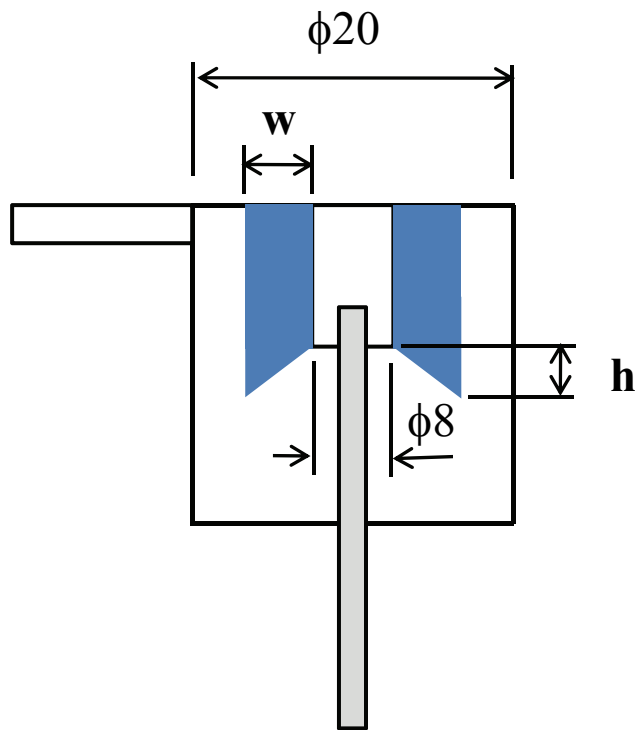


Fig.7 Effect of inlet flow rate and electrical potential on partial separation efficiency ($\Delta z=240\text{mm}$)



Dimensions of rings

Type	Type N	Type A	Type B
w[mm]	0	3	5
h [mm]	0	3	10

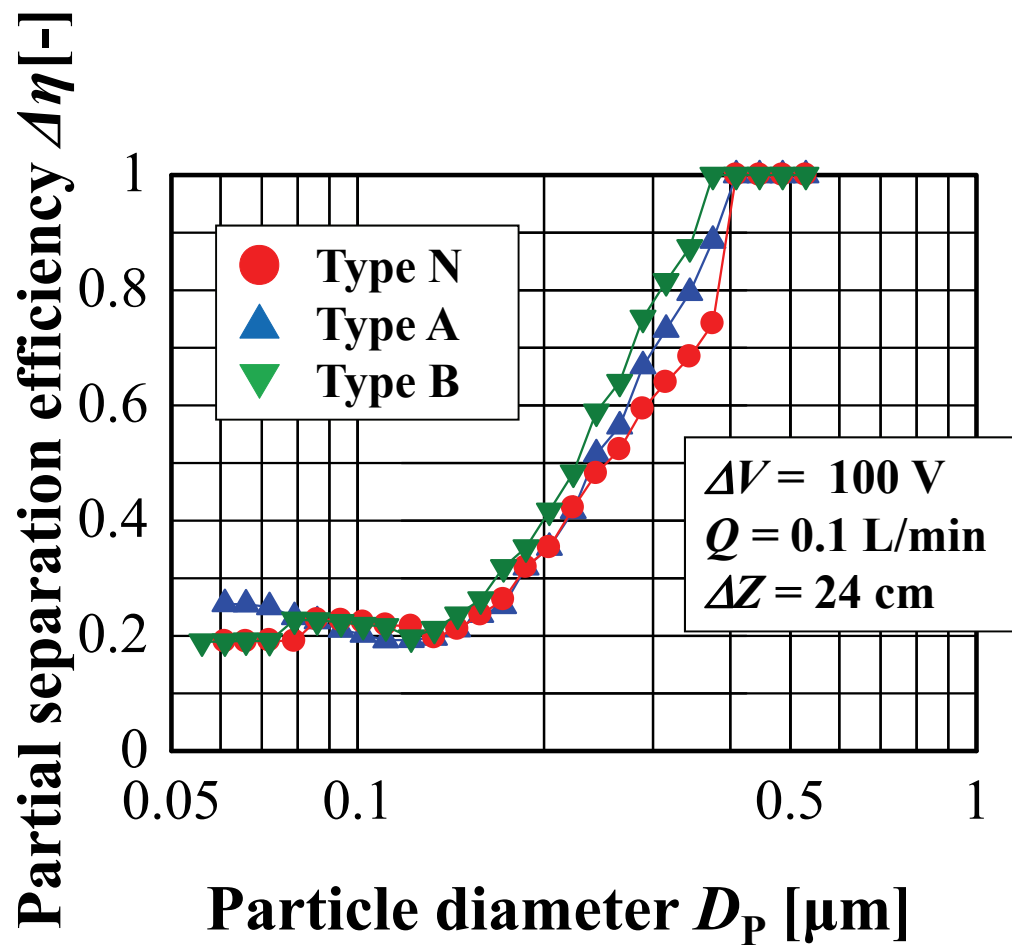


Fig.8 Effect of special ring attached on upper plate on partial separation efficiency

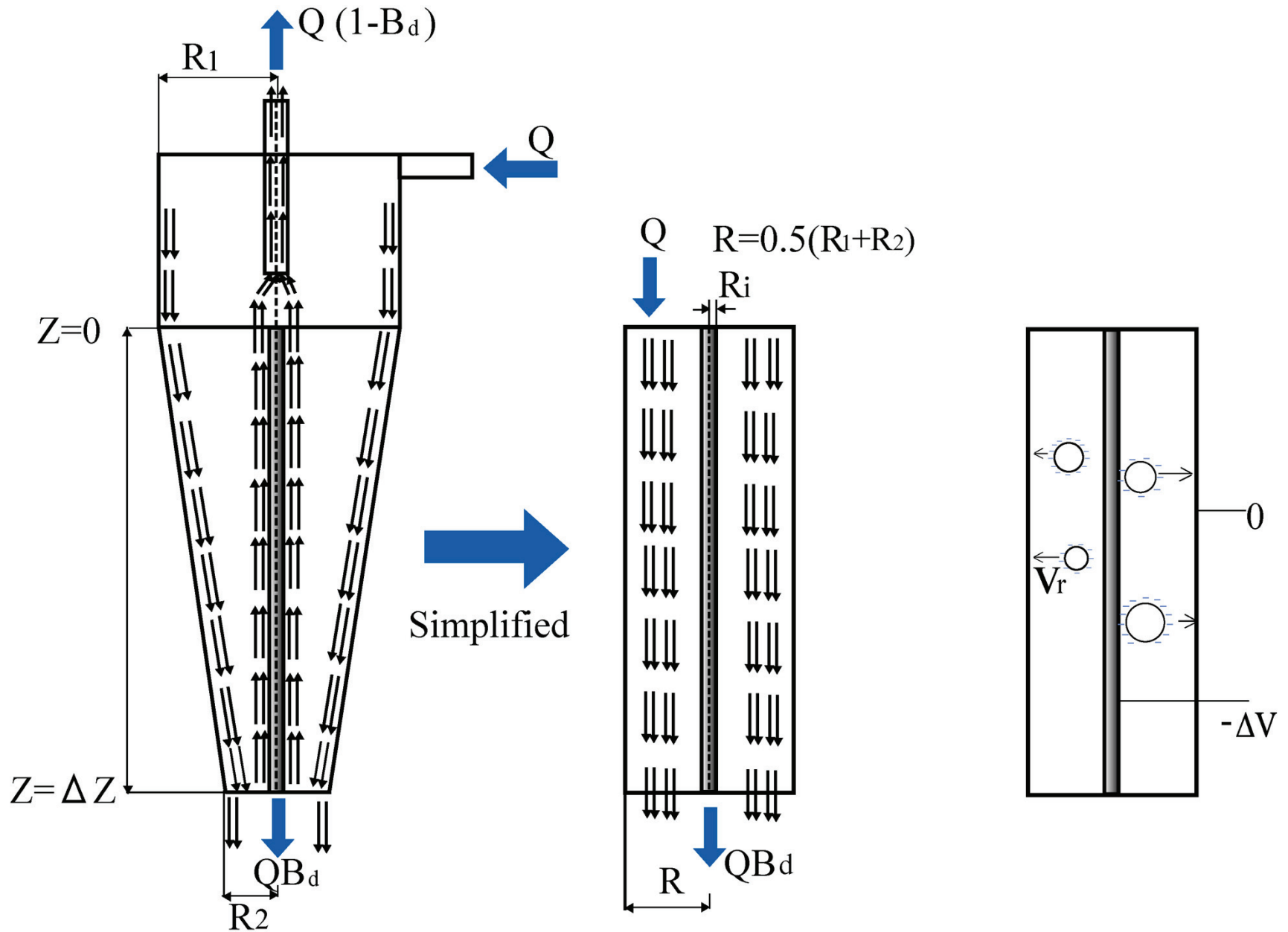


Fig. 9 Particle collection model of electrical hydro-cyclone and notations used in the proposed model

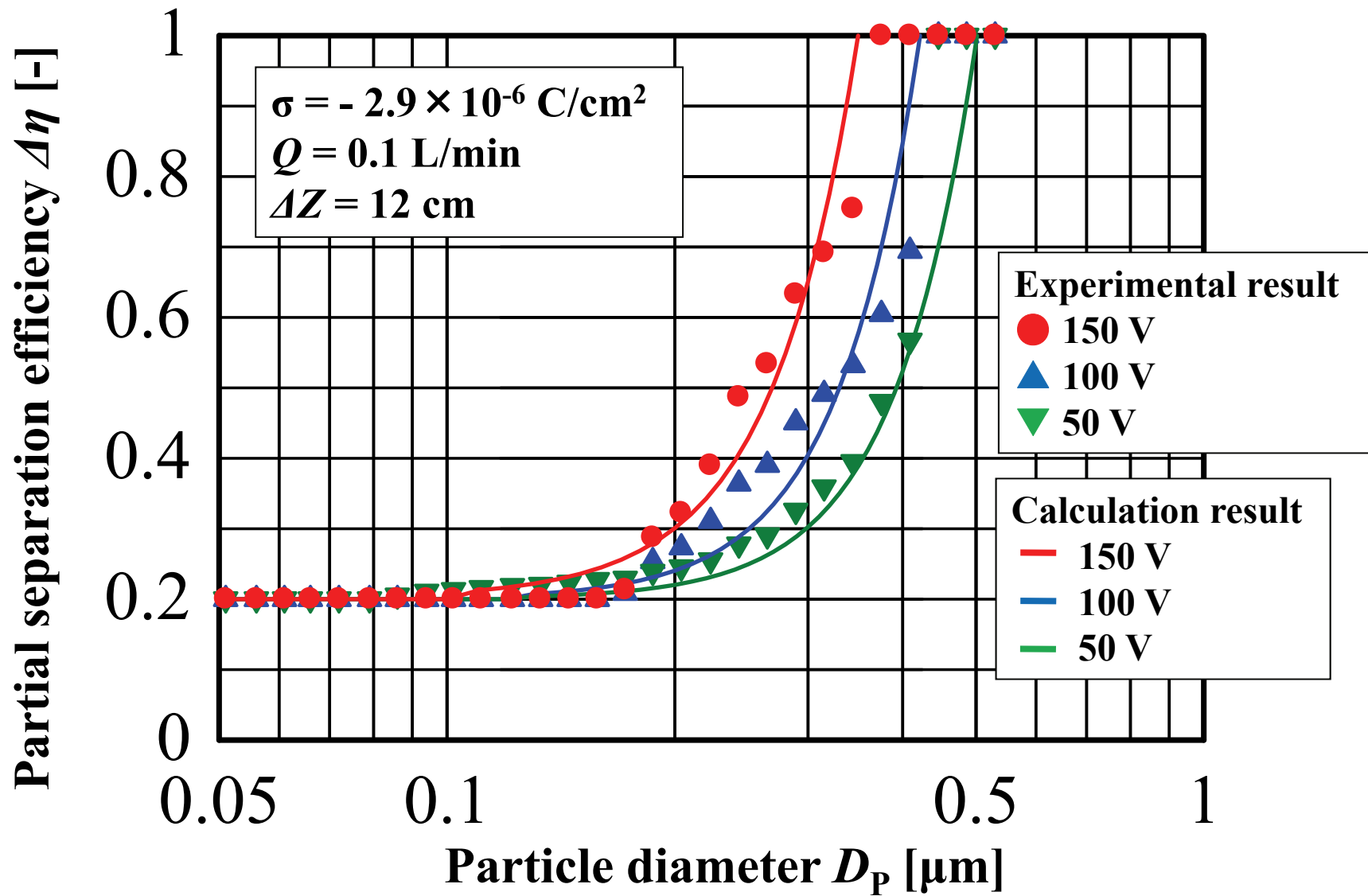


Fig.10-1 Effect of applied potential on partial separation efficiency
 ($\Delta z=120\text{mm}$)

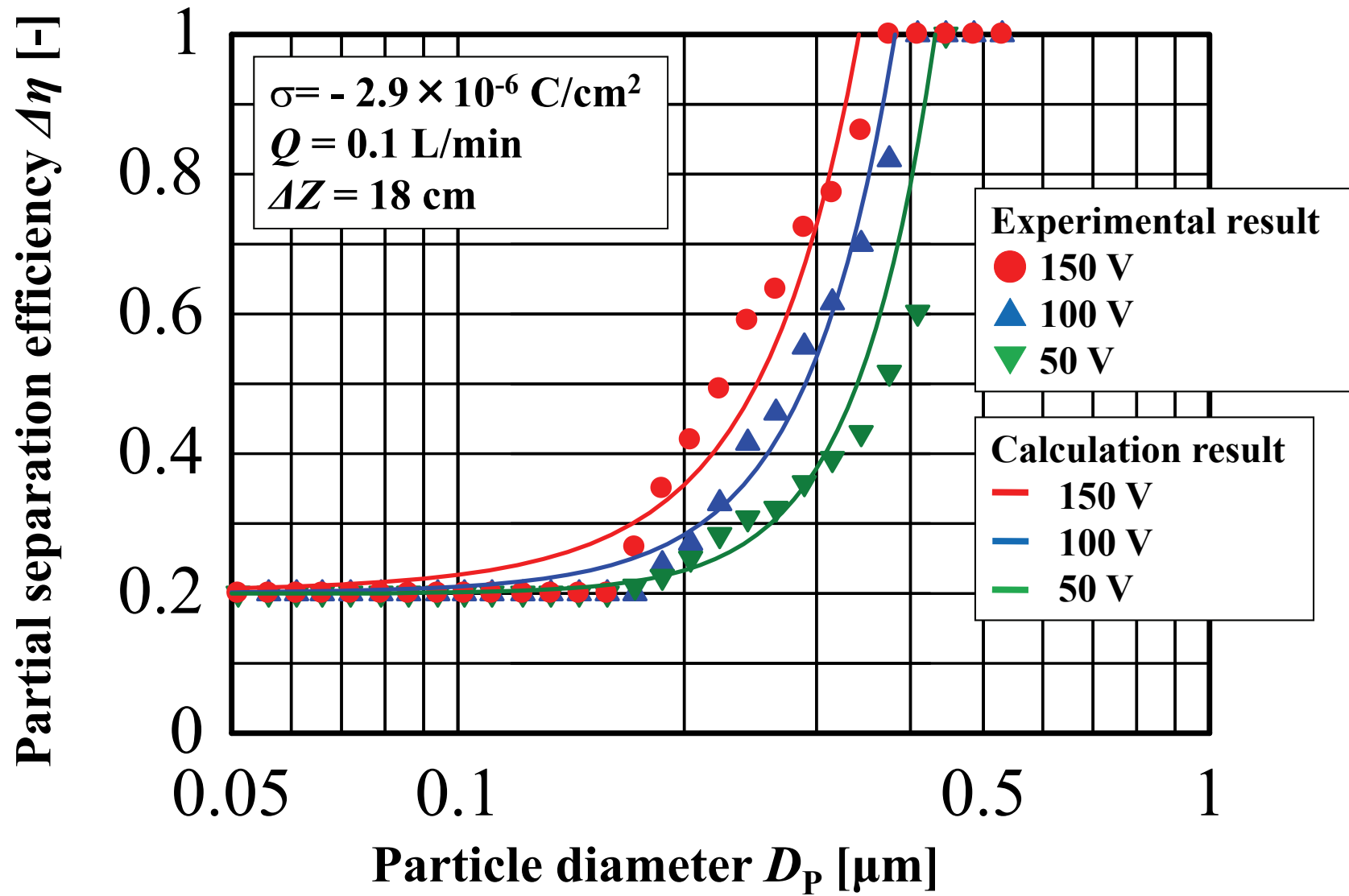


Fig.10-2 Effect of applied potential on partial separation efficiency
 ($\Delta z=180\text{mm}$)

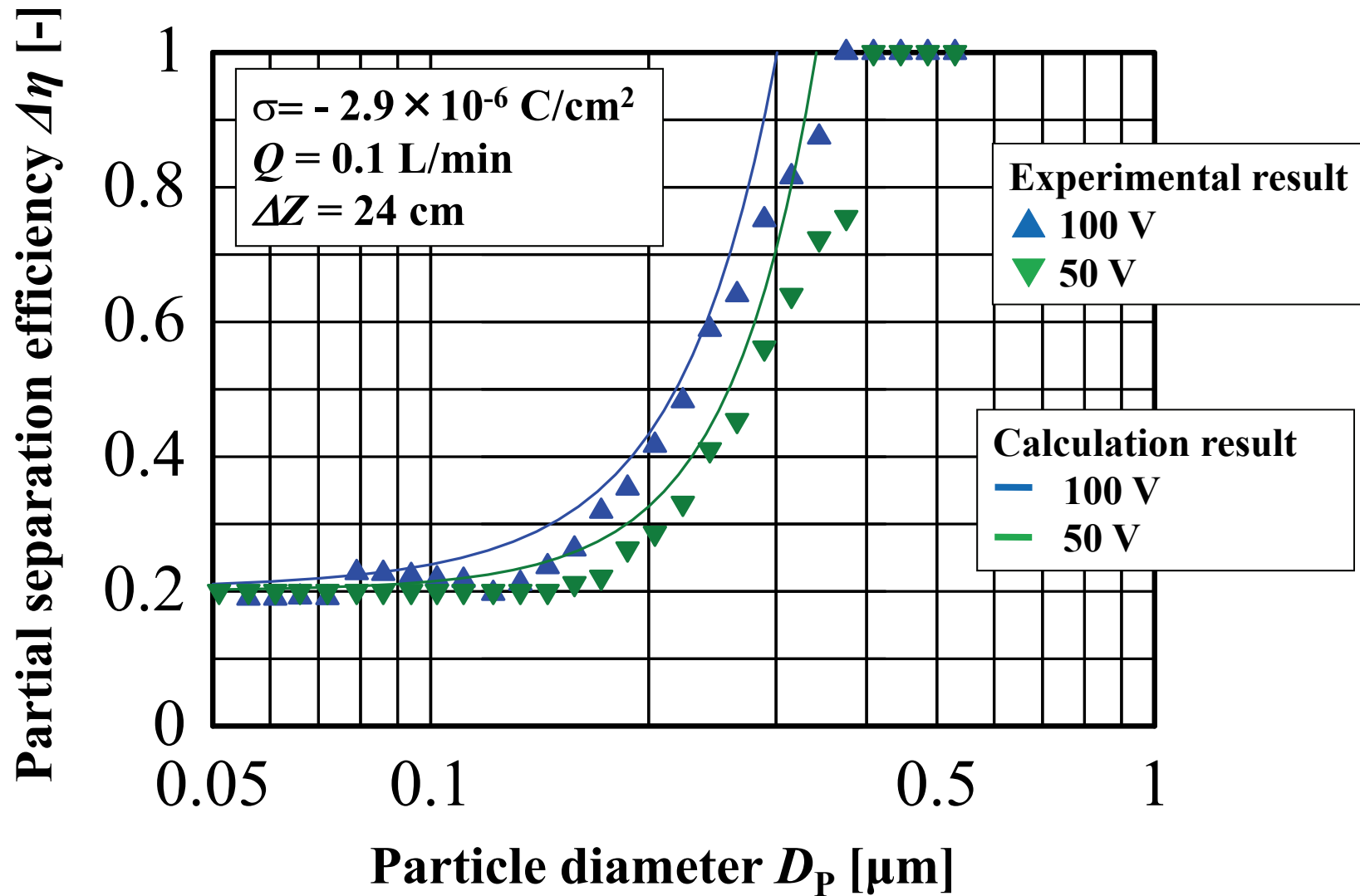


Fig.10-3 Effect of applied potential on partial separation efficiency ($\Delta z=240\text{mm}$)

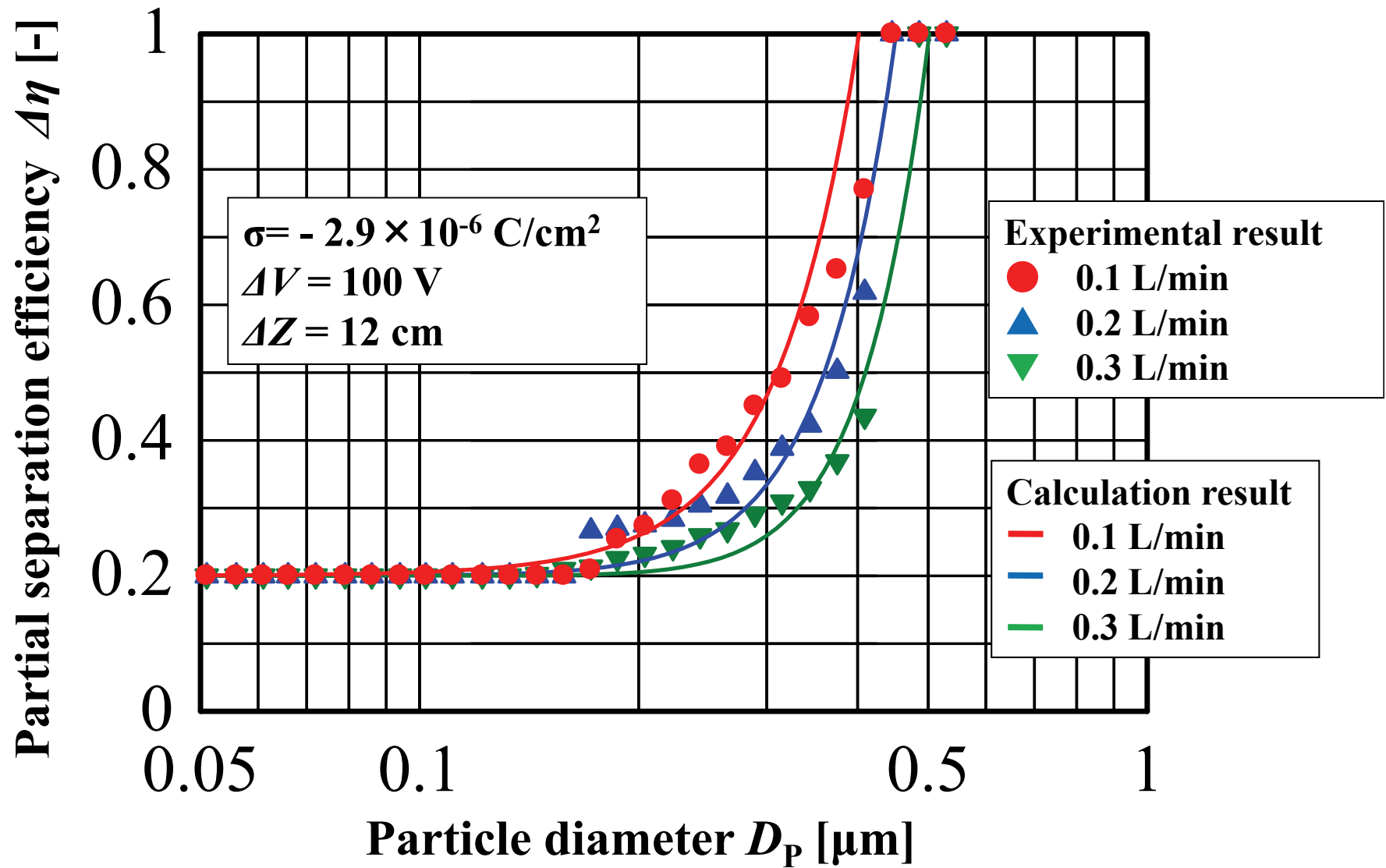


Fig.11-1 Effect of inlet flow rate on partial separation efficiency ($\Delta z=120\text{mm}$)

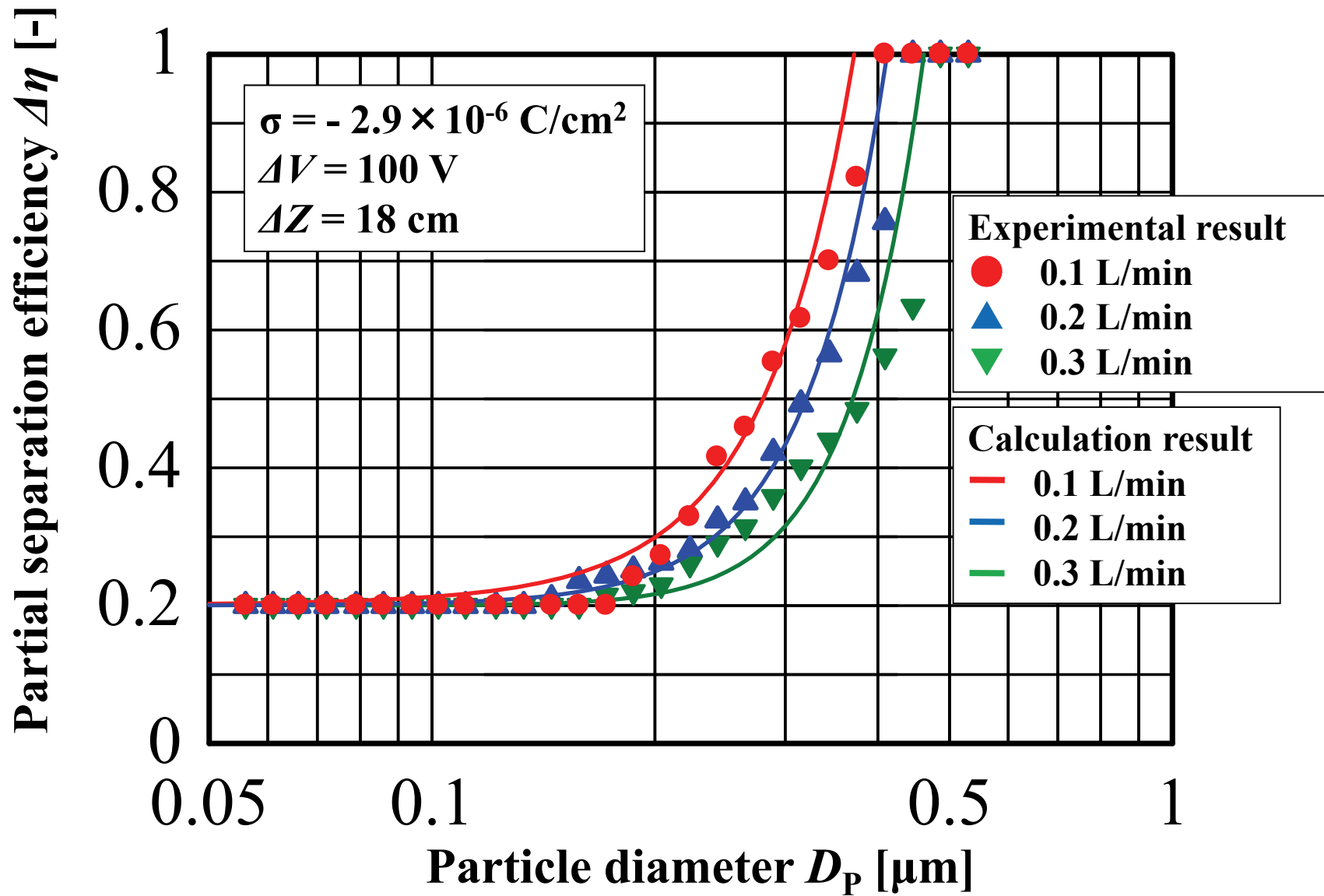


Fig.11-2 Effect of inlet flow rate on partial separation efficiency ($\Delta z=180\text{mm}$)

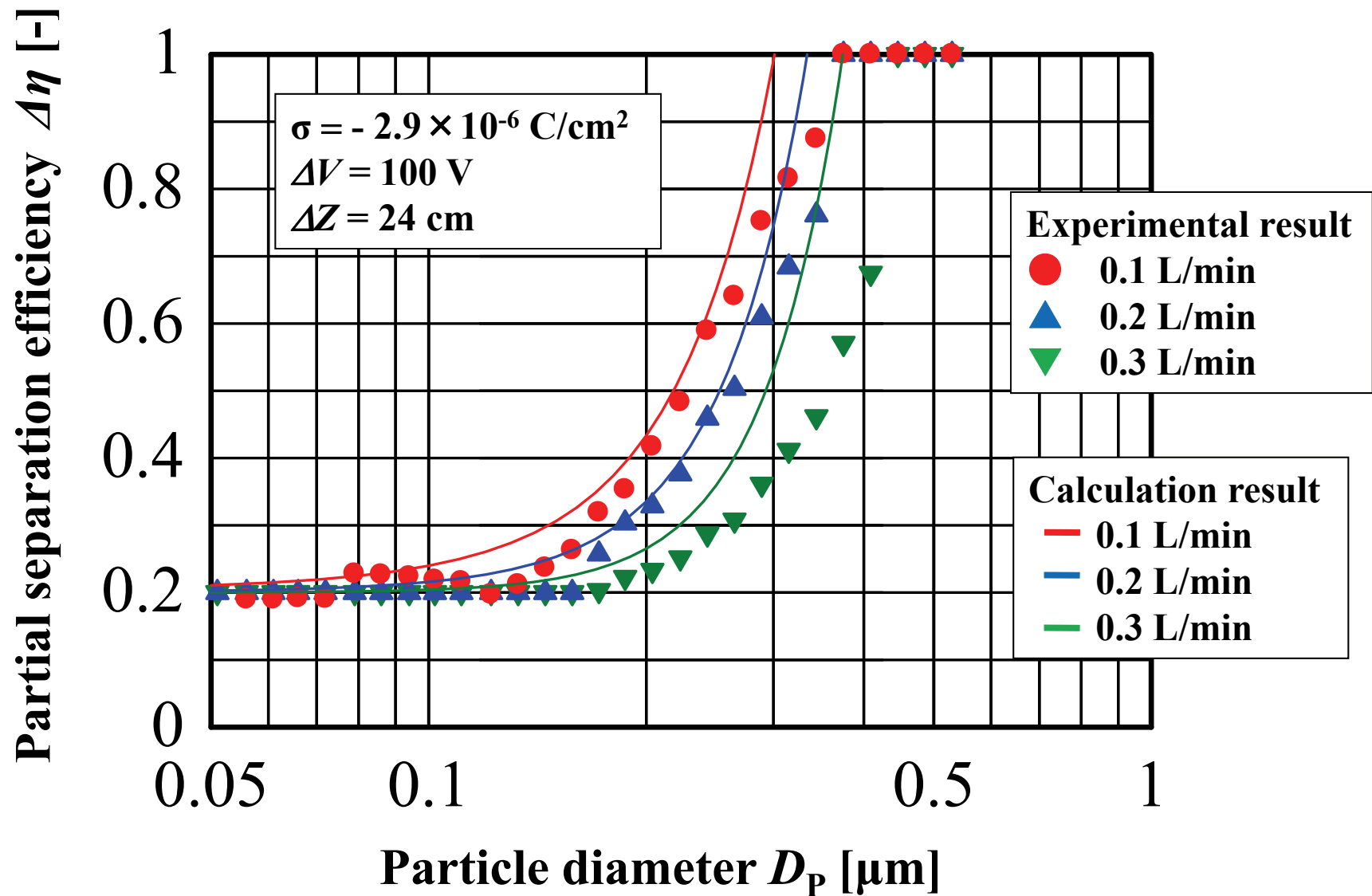


Fig.11-3 Effect of inlet flow rate on partial separation efficiency ($\Delta z=240\text{mm}$)

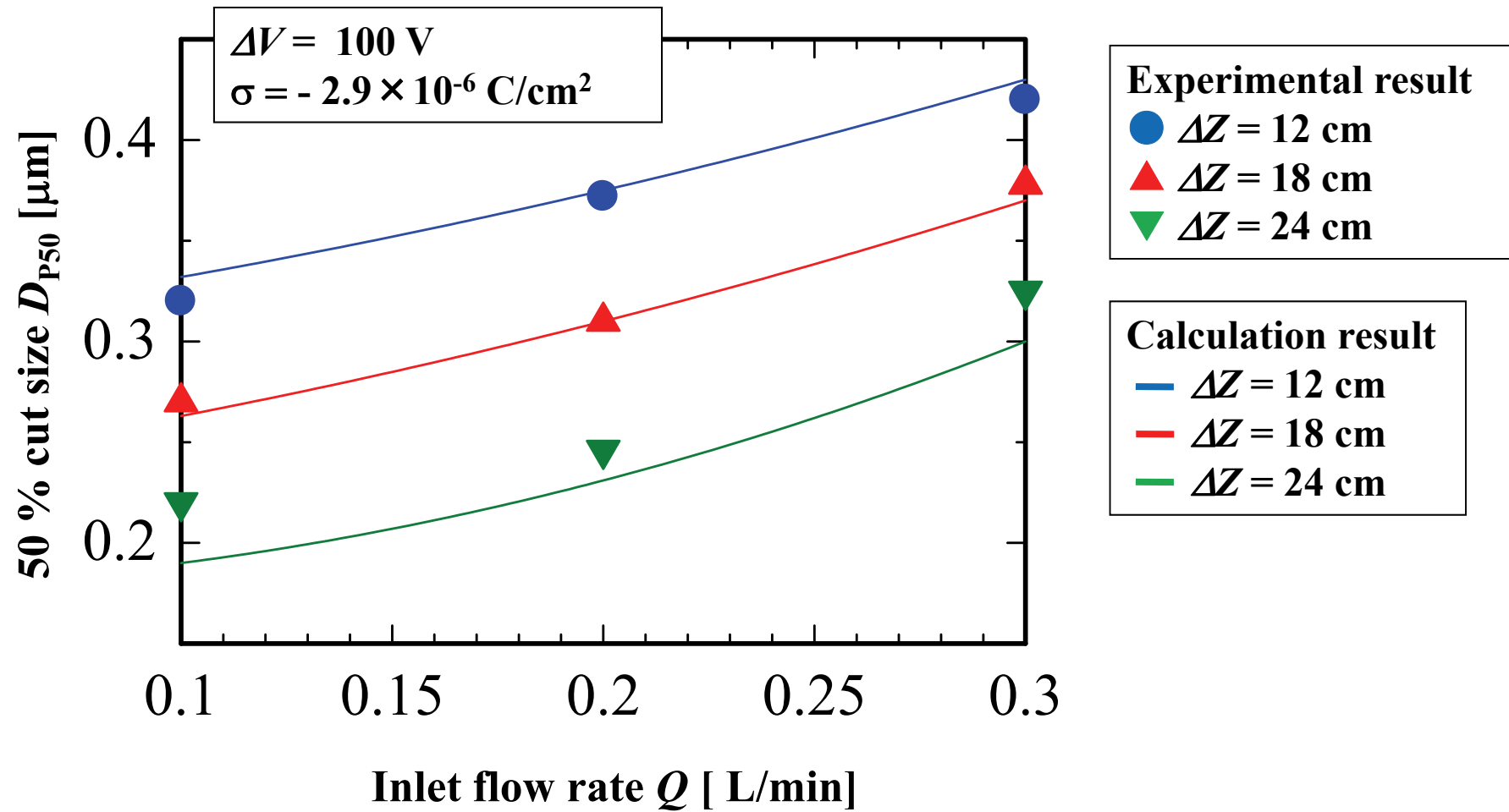


Fig.12 Relation between 50% cut size and inlet flow rate for various conical length